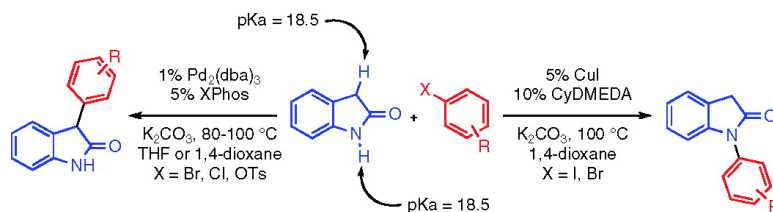


Orthogonal Pd- and Cu-Based Catalyst Systems for C- and N-Arylation of Oxindoles

Ryan A. Altman, Alan M. Hyde, Xiaohua Huang, and Stephen L. Buchwald

J. Am. Chem. Soc., **2008**, 130 (29), 9613-9620 • DOI: 10.1021/ja803179s • Publication Date (Web): 28 June 2008

Downloaded from <http://pubs.acs.org> on February 8, 2009



More About This Article

Additional resources and features associated with this article are available within the HTML version:

- Supporting Information
- Links to the 2 articles that cite this article, as of the time of this article download
- Access to high resolution figures
- Links to articles and content related to this article
- Copyright permission to reproduce figures and/or text from this article

[View the Full Text HTML](#)

Orthogonal Pd- and Cu-Based Catalyst Systems for C- and N-Arylation of Oxindoles

Ryan A. Altman, Alan M. Hyde, Xiaohua Huang, and Stephen L. Buchwald*

Department of Chemistry, Massachusetts Institute of Technology,
Cambridge, Massachusetts 02139

Received May 2, 2008; E-mail: sbuchwal@mit.edu

Abstract: In the cross-coupling reactions of unprotected oxindoles with aryl halides, Pd- and Cu-based catalyst systems displayed orthogonal chemoselectivity. A Pd-dialkylbiarylphosphine-based catalyst system chemoselectively arylated oxindole at the 3 position, while arylation occurred exclusively at the nitrogen using a Cu-diamine-based catalyst system. Computational examination of the relevant $L_1Pd(Ar)(oxindolate)$ and diamine-Cu(oxindolate) species was performed to gain mechanistic insight into the controlling features of the observed chemoselectivity.

Introduction

In recent years, Pd-catalyzed¹ and Cu-catalyzed² nucleophilic substitution reactions of aryl halides have been areas of intensive research. Our laboratory has been intimately involved in designing and developing highly efficient and user-friendly Pd- and Cu-based catalyst systems to cross-couple aryl halides with a wide variety of nucleophiles, including amides^{3,4} and ketone enolate derivatives.^{5,6}

Generally, Cu- and Pd-catalyzed arylation reactions of both linear and cyclic aliphatic amides react at the more acidic N-H moiety as opposed to the less acidic C-H_α position. For instance, when reacting 2-pyrrolidinone with aryl halides, both Cu-diamine- and Pd-biarylmonophosphine-based catalyst systems provide the N-aryl amide in excellent yield (Scheme 1).^{3,4} Ongoing work in our and other laboratories⁷ has identified oxindole as a unique substrate for chemoselective metal-catalyzed cross-coupling reactions with aryl halides. Because

of the identical acidities of the protons in positions C3 and N1 ($pK_a = 18.5$),⁸ the cross-coupling reactions of oxindole with aryl halides might provide either the C-aryl or the N-aryl products.

Importantly, N1-aryl and C3-aryl oxindole products of the type generated from the reactions described in this manuscript display interesting biological activities with therapeutic applications (Figure 1).⁹ In addition, the amide of the N-aryl oxindole can be cleaved to provide access to a variety of derivatives of 2-(2-phenylamino)phenyl)ethanoic acid nonsteroidal anti-inflammatory agents, such as Lumiracoxib¹⁰ and Diclofenac.¹¹

Herein, we describe improved reaction conditions for the Cu-catalyzed N1-arylation reaction with aryl iodides and bromides and general reaction conditions for the Pd-catalyzed C3-arylation reaction of unprotected oxindoles with aryl chlorides and tosylates. Further, we report computational studies that suggest reasonable explanations for the observed selectivity.

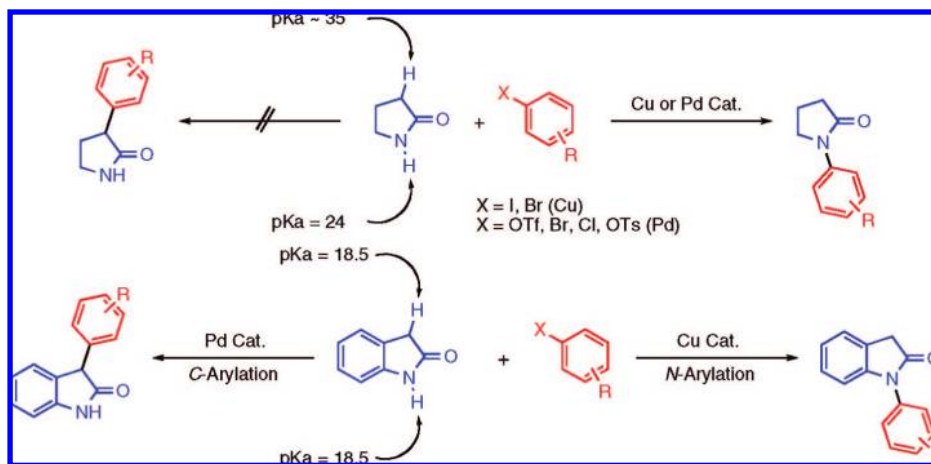
Results

Pd-Catalyzed C3-Arylation of Oxindoles. The use of 1% Pd₂(dba)₃ and 5% XPhos (Figure 2) was found to facilitate the

- (1) (a) Culkin, D. A.; Hartwig, J. F. *Acc. Chem. Res.* **2003**, *36*, 234. (b) Jiang, L.; Buchwald, S. L. Palladium-catalyzed aromatic carbon–nitrogen bond formation. In *Metal-Catalyzed Cross-Coupling Reactions*, 2nd ed.; de Meijere, A., Diederich, F., Eds.; Wiley-VCH: Weinheim, Germany, 2004; pp 699–760.
- (2) (a) Monnier, F.; Taillefer, M. *Angew. Chem., Int. Ed.* **2008**, *47*, 3096. (b) Beletskaya, I. P.; Chepravov, A. V. *Coord. Chem. Rev.* **2004**, 2337. (c) Ley, S. V.; Thomas, A. W. *Angew. Chem., Int. Ed.* **2003**, *42*, 5400. (d) Kunz, K.; Scholz, U.; Ganzer, D. *Synlett* **2003**, 2428.
- (3) For Cu-catalyzed N-arylation of amides using *N,N'*-dimethyl-1,2-ethylenediamine-derived ligands, see: (a) Klapars, A.; Antilla, J. C.; Huang, X.; Buchwald, S. L. *J. Am. Chem. Soc.* **2001**, *123*, 7727. (b) Klapars, A.; Huang, X.; Buchwald, S. L. *J. Am. Chem. Soc.* **2002**, *124*, 7421.
- (4) For Pd-catalyzed amidation of aryl halides using Xantphos and dialkylbiarylmonophosphine ligands, see: (a) Yin, J.; Buchwald, S. L. *J. Am. Chem. Soc.* **2002**, *124*, 6043. (b) Huang, X.; Anderson, K. W.; Zim, D.; Jiang, L.; Klapars, A.; Buchwald, S. L. *J. Am. Chem. Soc.* **2003**, *125*, 6653. (c) Ikawa, T.; Barder, T. E.; Biscoe, M. R.; Buchwald, S. L. *J. Am. Chem. Soc.* **2007**, *129*, 13001.
- (5) (a) Palucki, M.; Buchwald, S. L. *J. Am. Chem. Soc.* **1997**, *119*, 11108. (b) Fox, J. M.; Huang, X.; Chieffi, A.; Buchwald, S. L. *J. Am. Chem. Soc.* **2000**, *122*, 1360. (c) Hamada, T.; Chieffi, A.; Ahman, J.; Buchwald, S. L. *J. Am. Chem. Soc.* **2002**, *124*, 1261. (d) Nguyen, H. N.; Huang, X.; Buchwald, S. L. *J. Am. Chem. Soc.* **2003**, *125*, 11818.
- (6) Hennessy, E. J.; Buchwald, S. L. *Org. Lett.* **2002**, *4*, 269.

- (7) (a) Phillips, D. P.; Hudson, A. R.; Nguyen, B.; Lau, T. L.; McNeill, M. H.; Dalgard, J. E.; Chen, J. H.; Penuliar, R. J.; Miller, T. A.; Zhi, L. *Tetrahedron Lett.* **2006**, *47*, 7137. (b) Huang, J.; Bunel, E.; Faul, M. M. *Org. Lett.* **2007**, *9*, 4343. (c) Durbin, M. J.; Willis, M. C. *Org. Lett.* **2008**, *10*, 1413. (d) van den Hoogenband, A.; Lange, J. H. M.; Iwema-Bakker, W. I.; den Hartog, J. A. J.; van Schaik, J.; Feenstra, R. W.; Terpstra, J. W. *Tetrahedron Lett.* **2006**, *47*, 4361.
- (8) Bordwell, F. G.; Fried, H. E. *J. Org. Chem.* **1991**, *56*, 4218.
- (9) (a) Luk, K. C.; So, S. S.; Zhang, J.; Zhang, Z. (F. Hoffman-LaRoche AG) Oxindole Derivatives. WO 2006/136606 A3, December 28, 2006. (b) Hewawasam, P.; Gribkoff, V. K.; Pendri, Y.; Dworetzky, S. I.; Meanwell, N. A.; Martinez, E.; Boissard, C. G.; Post-Munson, D. J.; Trojnacki, J. T.; Yeleswaram, K.; Pajor, L. M.; Knipe, J.; Gao, Q.; Perrone, R.; Starrett, J. E., Jr. *Bioorg. Med. Chem. Lett.* **2002**, *12*, 1023. (c) Sarges, R.; Howard, H. R.; Koe, K.; Weissman, A. *J. Med. Chem.* **1989**, *32*, 437.
- (10) Karnachi, A. A.; Bateman, S. D. (Novartis-AG) Pharmaceutical Composition Comprising Lumiracoxib. WO 03/020261 A1, March 13, 2003.
- (11) Acemoglu, M.; Allmendinger, T.; Calienni, J.; Cercus, J.; Loiseleur, O.; Sedelmier, G. H.; Xu, D. *Tetrahedron* **2004**, *60*, 11571.

Scheme 1. Pd- and Cu-Catalyzed C- and N-Arylation of 2-Pyrrolidinone and Oxindole



cross-coupling of aryl chlorides with oxindoles unsubstituted at C3 using K_2CO_3 as the base in THF or 1,4-dioxane at temperatures ranging between 80 and 100 °C (Table 1). The use of bidentate or other dialkylbiarylmonophosphine ligands provided a low conversion of starting material and yield of products. The Pd-catalyzed C3-arylation reaction of oxindoles with aryl chlorides tolerated a variety of functional groups on the meta and para positions of the electrophile (Table 1, entries 1–10); however, ortho-substituted aryl chlorides provided a low conversion of reactants (>5%) even at slightly elevated temperatures (up to 120 °C) with a variety of biarylmonophosphine ligands. Under the standard reaction conditions, the use of 3-chlorobenzonitrile provided low yields of coupled product due

to partial hydrolysis of the nitrile functional group to an amide (Table 1, entry 4). This side reaction could be partially impeded by the addition of activated 4 Å molecular sieves to the reaction vessel. Using *t*-BuOH as a solvent, an unactivated aryl benzenesulfonate could be successfully cross-coupled to provide the C-aryl product in modest yield (Table 1, entry 5). Substrates possessing substituents on the benzannulated backbone (Table 1, entries 6–8) as well as on the nitrogen atom (Table 1, entries 9–10) provided more highly substituted products. Using XPhos as a ligand, the reaction of a 3-substituted oxindole was unsuccessful;^{7b} however, using reoptimized reaction conditions (RuPhos/NaOt-Bu/toluene), the cross-coupling reactions of 3-methyl- and 3-benzoyloxindole were successfully accomplished to generate quaternary stereocenters at the C3 positions to produce racemic products (Table 1, entries 11–12). In contrast to the previously reported catalyst systems for the C3-vinylation of unprotected oxindoles and C3-arylation of protected oxindoles, which required strong bases such as potassium bis(trimethylsilyl)amide (KHMSD) and Lithium bis(trimethylsilyl)amide (LHMDS), respectively, for the reactions to proceed,^{7b,c} K_2CO_3 and NaOt-Bu were found to be suitable bases with our catalyst system.

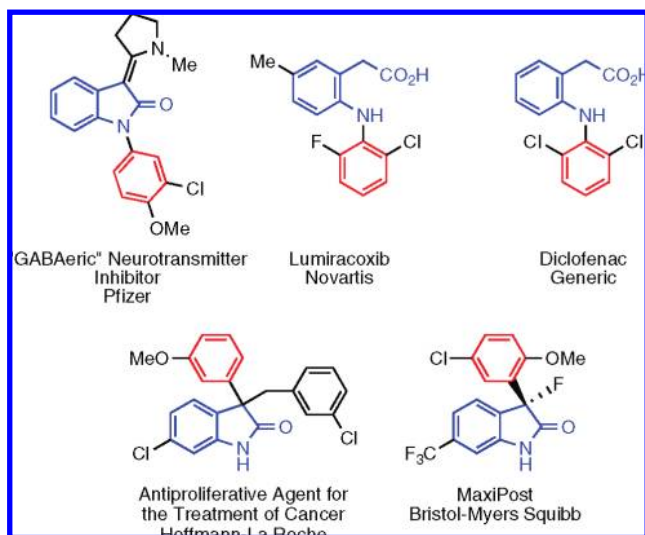


Figure 1. Therapeutically relevant C-aryl and N-aryl oxindoles and related compounds.

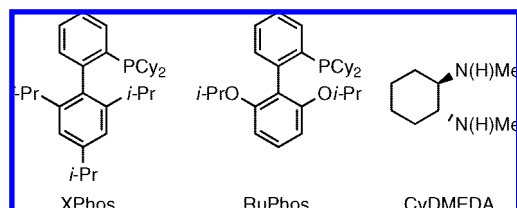
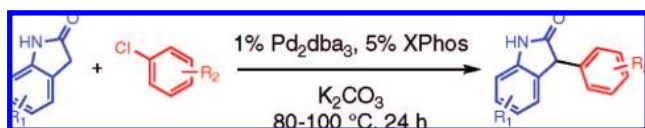


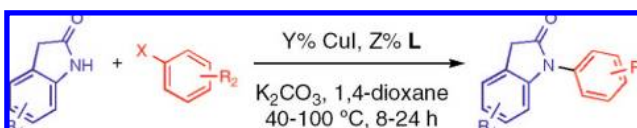
Figure 2. Ligands employed for metal-catalyzed C- and N-arylation of oxindole.

Cu-Catalyzed N-Arylation of Oxindoles. The Cu-catalyzed N-arylation reactions of meta- and para-substituted aryl iodides generally proceeded smoothly at temperatures ranging from 80 to 100 °C using 1–5% catalyst loading, 4–10% *trans*-*N,N'*-dimethylcyclohexane-1,2-diamine (CyDMEDA) (Figure 2) as the ligand, K_2CO_3 as the base, and 1,4-dioxane as the solvent (Table 2, entries 1–8). In these reactions, the C3-aryl product was not detected by GC-MS analysis of the crude reaction mixtures. Using this catalyst system, ortho-substituted aryl iodides were unreactive, even at temperatures up to 150 °C in high boiling-point solvents. This serves to reinforce the notion that ortho-substituted aryl halides can be quite difficult to activate in Cu-catalyzed C-heteroatom bond-forming reactions. At 60–100 °C, the cross-coupling reaction of 1-bromo-4-iodobenzene with oxindole provided a complex mixture of products; however, by lowering the reaction temperature to 40 °C, the bromide-containing product could be isolated in acceptable yield (Table 2, entry 3). The addition of activated 4 Å molecular sieves to the reaction mixtures was necessary for substrates containing hydroxide- or water-sensitive functional groups (Table 2, entries 4 and 7). As anticipated, substituents on the nucleophile also were tolerated (Table 2, entries 6–7).

Table 1. Pd-Catalyzed C-Arylation of Oxindoles^a

entry	product	solvent	temp. (°C)	% yield
1		THF	80	92
2		1,4-dioxane	100	81
3		1,4-dioxane	100	89 ^b
4		THF	80	55 ^c
5		<i>t</i> -BuOH	110	67 ^d
6		1,4-dioxane	100	80
7		THF	80	77
8		THF	80	63
9		THF	80	82
10		1,4-dioxane	80	94 ^e
11		toluene	100	90 ^f
12		toluene	100	90 ^g

^a Reactions conditions: 1.0–1.2 mmol of oxindole, 1.2–1.0 mmol of ArCl, 2.0 mmol of K₂CO₃, 0.010 mmol of Pd₂dba₃, 0.050 mmol of XPhos, and 1.0 mL of solvent in a sealed tube under Ar atmosphere. Yields reported are an average of at least two runs determined to be >95% pure by elemental analysis or ¹H NMR. ^b 3.0 mmol of K₂CO₃. ^c 4 Å mol sieves. ^d From ArOSO₂Ph. ^e K₃PO₄ used as base. ^f From ArBr. RuPhos and NaOt-Bu employed as ligand and base; 9 h reaction time. ^g From ArBr. RuPhos and NaOt-Bu employed as ligand and base; 20 h reaction time.

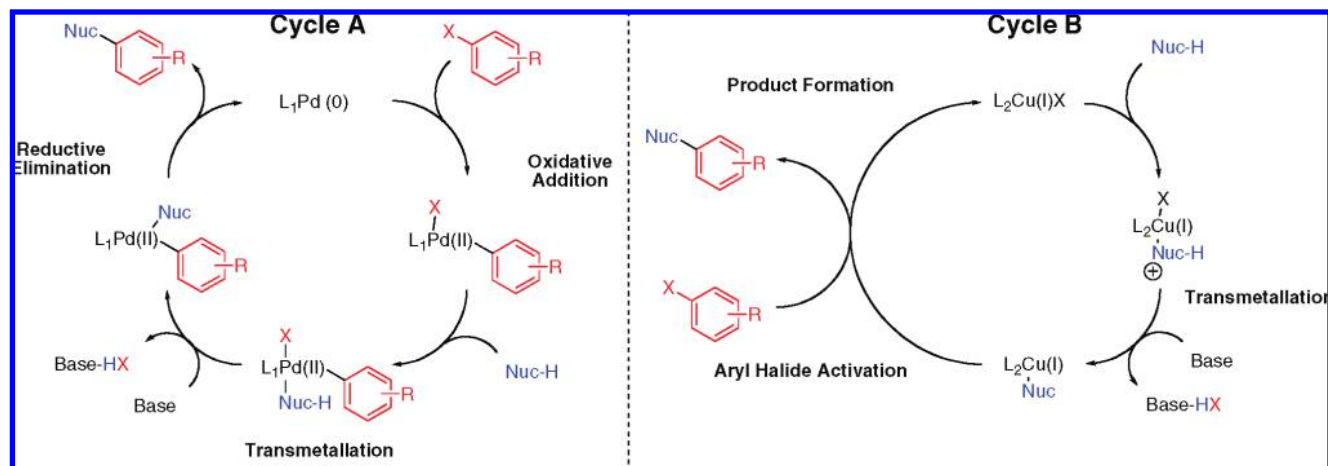
Table 2. Cu-Catalyzed N-Arylation of Oxindoles^a

entry	product	Y	X	Z	temp. (°C)	% yield
1		5	I	10	100	86
2		1	I	4	100	94
3		5	I	10	40	61
4		5	I	10	80	72 ^b
5		1	I	4	80	85
6		5	I	10	80	69
7		5	I	10	80	87 ^b
8		10	Br	20	100	62
9		10	Br	20	100	71
10		10	Br	20	100	77
11		10	Br	20	100	72

^a Reactions conditions: 1.0–1.2 mmol of oxindole, 1.2–1.0 mmol of ArI, 2.0 mmol of K₂CO₃, and 1.0 mL of 1,4-dioxane in a sealed tube under Ar atmosphere. Yields reported are an average of at least two runs determined to be >95% pure by elemental analysis or ¹H NMR. ^b 4 Å mol sieves.

Aryl bromides also proved to be reactive in the Cu-catalyzed cross-coupling reactions with oxindoles (Table 2, entries 8–11), although higher catalyst loadings were necessary to ensure full conversion of the substrates within a 24 h time period. Although the C3-aryl oxindole product was not observed, up to 5% of the N1,C3-bis-arylated product (10% aryl halide consumption) was isolated in the reaction of 5-bromo-*m*-xylene (Table 2, entry 9). A second common side product, when using aryl bromides, was the reduced arene. Aryl chlorides were not suitable coupling

Scheme 2. Mechanisms of Pd- and Cu-Catalyzed Nucleophilic Substitution Reactions of Aryl Halides



partners for this reaction. These substrates are generally unreactive in Cu-catalyzed C-heteroatom bond-forming reactions due to the high energy required for activating the $C_{\text{aryl}}\text{-Cl}$ bond relative to the $-\text{Br}$ or $-\text{I}$ bonds.²

Computational Studies of Ligand-Metal(Oxindole) Complexes.

The catalytic cycle of Pd-catalyzed nucleophilic substitution reactions of aryl halides involves three steps: (1) oxidative-addition, (2) transmetalation, and (3) reductive-elimination (Scheme 2, Cycle A).¹

Since oxindole does not participate in the oxidative-addition step of the cycle, the selectivity-controlling feature for the Pd-based catalyst system must involve either transmetalation or reductive-elimination. To gain further insight into the observed selectivity, the relative energies and structures of various $L_1Pd(\text{Ph})(\text{oxindolate})$ complexes were calculated by DFT methods (Figures 3 and 4; see Computational Methods for full details).

In light of the experimental findings that catalysts derived from XPhos were the ones that produced high yields of the C3-

arylated oxindole product, it was critical to model structures that contained the entire ligand without any approximations. The geometry of the $\text{XPhos} \cdot \text{Pd}(\text{Ph})(\text{oxindolate})$ complex formed following transmetalation was minimized with the Pd bound to either the nitrogen or the α -carbon of the oxindole (Figure 3). This minimization was performed with structures in which the Pd points toward or away from the lower biaryl ring. Consistent with previous computational studies from our group,¹² three-coordinate $\text{Pd}(\text{II})/\text{dialkylbiarylmonophosphine}$ intermediates prefer the orientation shown in structures **1** and **2** with the Pd sitting above the lower biaryl ring. In both cases, the C-bound oxindolate was significantly higher in energy than the N-bound complex. This energy difference was 4.8 kcal/mol between **1** and **2** and 7.0 kcal/mol between **3** and **4**. We then determined the energies of the κ^2 -amidate (**5** and **9**), O-bound amidate and enolate (**6**, **7**, **10**, and **11**), and η^3 -oxyallyl (**8** and **12**) structures, as they may be intermediates in the N to C isomerization process (Figure 4). As expected, the three-coordinate O-bound enolate and amidate structures are lower in energy when the Pd is pointing toward the lower ring. However, the four-coordinate κ^2 -amidate- and η^3 -oxyallyl-bound structures are lower in energy when the Pd is distal to the lower ring.

If the N- and C-bound structures exist in rapid equilibrium, then the barriers for reductive-elimination should be product determining. Thus, transition states for both C–C and C–N reductive-elimination processes were calculated (Figure 5). The mechanism for reductive-elimination from Pd-bound enolates has not been well-studied and could occur by different mechanisms involving O-bound, C-bound, or η^3 -oxyallyl Pd intermediates. Hartwig and Culkin¹³ put forth circumstantial evidence in support of a simple reduction-elimination between an η^1 -bound enolate and an arene. However, these studies were primarily performed using bidentate ligands, which may prevent η^3 -bound intermediates and relevant transition states. Several reports have appeared that indicate that η^3 -oxyallyl Pd intermediates may be involved in some Pd-enolate-based processes.¹⁴

Reasonable starting geometries for the transition states of enolate C–C reductive-elimination were arrived at by examining calculations reported by others for methyl-methyl reductive-

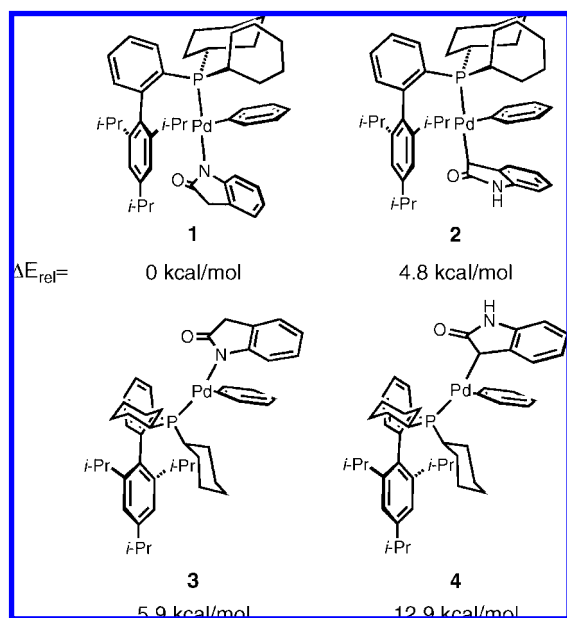


Figure 3. Calculated geometries and energies of C- and N-bound $\text{XPhos} \cdot \text{Pd}(\text{Ph})(\text{oxindolate})$ complexes with B3LYP (calculated at 298 K in THF).

(12) Barder, T. E.; Buchwald, S. L. *J. Am. Chem. Soc.* **2007**, *129*, 12003.
 (13) (a) Culkin, D. A.; Hartwig, J. F. *J. Am. Chem. Soc.* **2001**, *123*, 5816.
 (b) Culkin, D. A.; Hartwig, J. F. *Organometallics* **2004**, *23*, 3398.

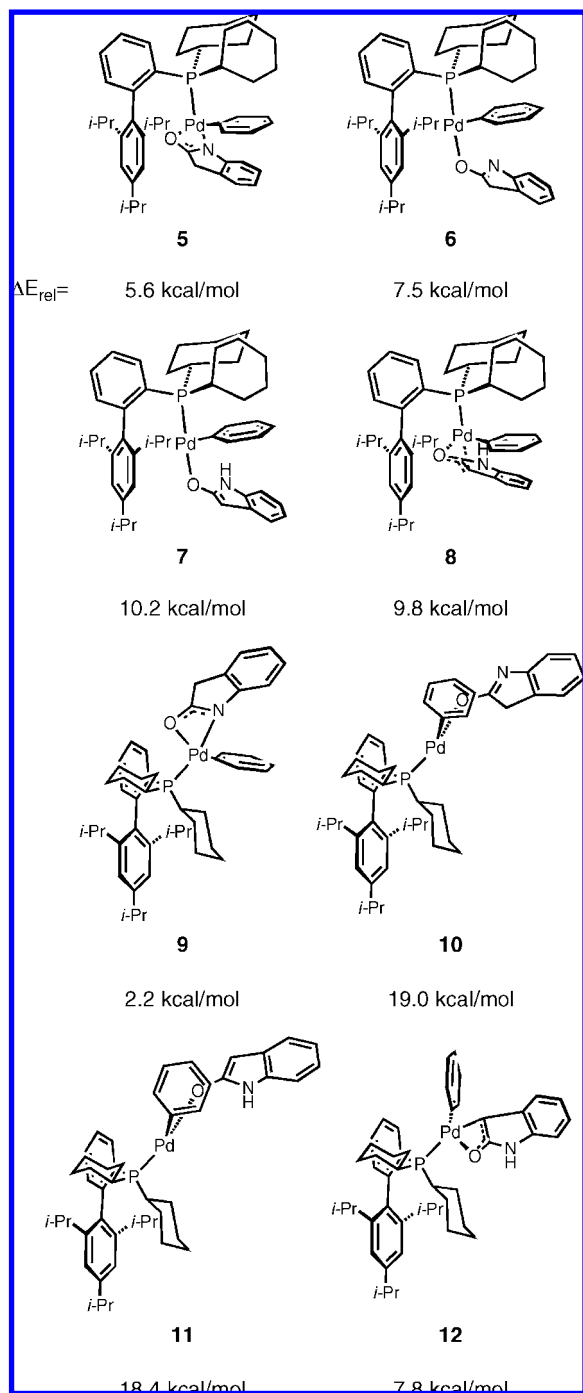


Figure 4. Calculated geometries and energies of the κ^2 -O- and η^3 -oxyallyl-bound XPhos·Pd(Ph)(oxindolate) complexes with B3LYP (calculated at 298 K in THF). ΔE_{rel} values are relative to complex **1** in Figure 3.

elimination from Pd.¹⁵ A prior publication by our group on the mechanism of aryl amination provided us with reasonable

- (14) (a) Ito, Y.; Nakatsuka, M.; Kise, N.; Saegusa, T. *Tetrahedron Lett.* **1980**, *21*, 2873. (b) Sodeoka, M.; Ohrai, K.; Shibasaki, M. *J. Org. Chem.* **1995**, *60*, 2648. (c) Albéniz, A. C.; Catalina, N. M.; Espinet, P.; Redón, R. *Organometallics* **1999**, *18*, 5571. (d) For a DFT study that reports an η^3 -oxyallyl Pd transition state between O- and C-bound enolates, see: Cámpora, J.; Maya, C. M.; Palma, P.; Carmona, E.; Gutiérrez, E.; Ruiz, C.; Graiff, C.; Tiripicchio, A. *Chem.—Eur. J.* **2005**, *11*, 6889.
- (15) (a) Low, J. J.; Goddard, W. A. *J. Am. Chem. Soc.* **1984**, *106*, 8321. (b) Ananikov, V. P.; Musaev, D. G.; Morokuma, K. *Organometallics* **2005**, *24*, 715.

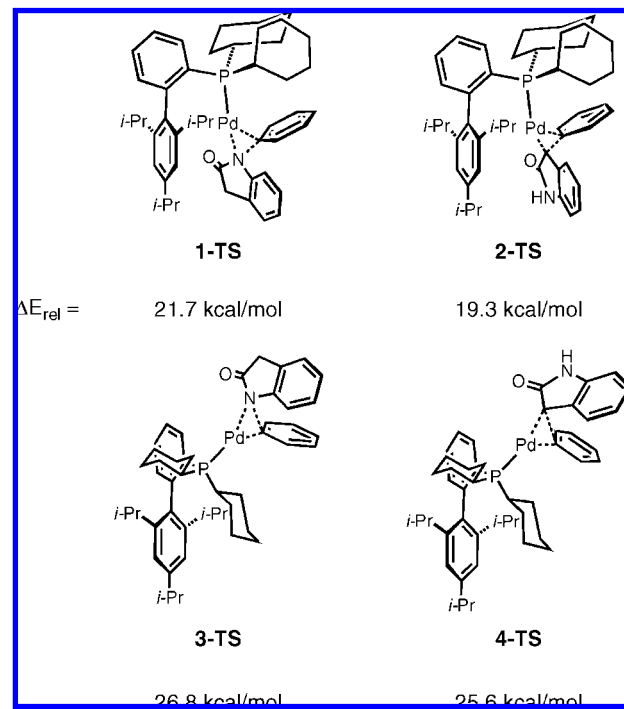


Figure 5. Calculated reductive-elimination transition states for XPhos·Pd(Ph)(oxindolate) with B3LYP (calculated at 298 K in THF). ΔE_{rel} values are relative to complex **1** in Figure 3.

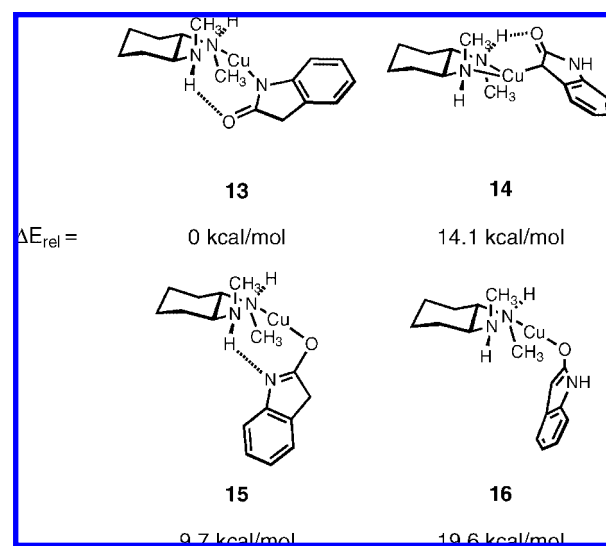
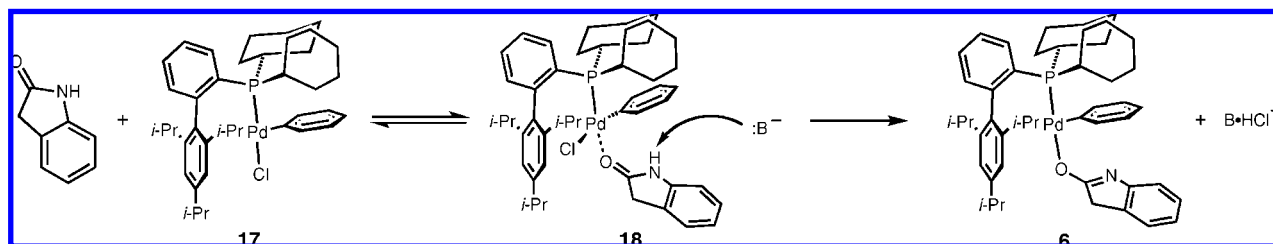


Figure 6. Calculated geometries and energies of CyDMEDA·Cu(oxindolate) complexes with B3LYP (calculated at 298 K).

starting geometries for amidate C–N reductive-elimination.¹² We were then able to quickly find transition states for both C–C and C–N reductive-elimination toward and away from the lower biaryl ring. ΔE^\ddagger for **1** \rightarrow **1-TS** was calculated to be 21.7 kcal/mol, while ΔE^\ddagger for **2** \rightarrow **2-TS** was significantly less at 14.5 kcal/mol. For structures with the Pd swung away, ΔE^\ddagger of **3** \rightarrow **3-TS** was calculated to be 20.9 kcal/mol, and ΔE^\ddagger of **4** \rightarrow **4-TS** was 12.6 kcal/mol. Although these barriers are lower than when the Pd is pointed toward the lower biaryl ring, their absolute energies are much higher. Therefore, it is unlikely that **3-TS** and **4-TS** contribute to the reaction course. We also attempted to find a transition state for C–C reductive-elimination, which proceeds through an η^3 pathway, but one could not be located.

Scheme 3. Transmetalation of Oxindole to XPhos·Pd(Ph)(Cl)



Cu-catalyzed amidation reactions of aryl halides initiate by addition of the nucleophile to a $L_2Cu(I)X$ complex to provide an $L_2Cu(I)$ amidate, followed by aryl halide activation and subsequent product formation.^{16,17} Although Guo et al. recently published a computational study that calculates the transition states and intermediates of the catalytic cycle for the Goldberg reaction,¹⁸ this study only considered a mechanism based on an insertion reaction between an $L_2Cu(I)$ (amidate) and an aryl halide to generate an $L_2Cu(III)$ -(Ar)(X)(amidate) species and neglected to evaluate evidence that an electron-transfer mechanism might be occurring, as suggested by Hida et al.¹⁹ Therefore, we assume that the mechanism of the rate-limiting aryl halide activation step is yet to be fully elucidated (Scheme 2, Cycle B). According to this paradigm, reaction of a molecule of oxindole with the CyDMEDA-CuI complex and base may provide multiple regioisomeric products, which could react with aryl halides to provide the *N*-aryl and *C3*-aryl products, respectively. To gain insight into the features that control the selectivity of the reaction, the energies of relevant CyDMEDA-Cu(I)(oxindolate) complexes were examined (Figure 6).

As observed with the Pd-based catalyst system, the *N*-bound (CyDMEDA)·Cu(oxindolate) **13** was found to be significantly lower in energy than both *C3*-bound and *O*-bound structures. In this structure, the geometry around Cu is a distorted T-shape, consistent with known neutral tricoordinate Cu(I) structures.²⁰ Interestingly, the calculation predicts a hydrogen bonding interaction between the carbonyl and one hydrogen of the amine (*O*–*H* distance of 1.9 Å). The *C3*-bound oxindolate **14** is significantly higher in energy by 14.1 kcal/mol. It is noteworthy that the geometry about Cu is no longer planar but trigonal pyramidal and equidistant to both nitrogen atoms. There also appears to be a hydrogen bond between the carbonyl oxygen and the amine hydrogen (*O*–*H* distance of 2.0 Å). The *O*-bound amidate **15** and enolate **16** are 9.3 and 19.2 kcal/mol higher in energy, respectively, than the *N*-bound structure. We also optimized κ^2 -amidate and η^3 -oxyallyl-bound structures, but no reasonable stationary points were found.

Discussion

In metal-catalyzed amidation reactions of aliphatic amides, such as 2-pyrrolidinone, coordination and deprotonation of the

nucleophile during the transmetalation step of the catalytic cycle occur at the more acidic *N*–*H* position as opposed to the less acidic *C*–*H*_α position (Scheme 1). In the case of oxindole, both the *N*–*H* and the *C*–*H*_α protons are significantly acidified due to the conjugation of the deprotonated anion with the aromatic ring. Further, the predisposition for the anion to reside on the more electronegative nitrogen atom is overcome by the aromatic stabilization gained from isomerization of the anion to generate an enolate.⁸ Thus, a 1:1 ratio of amidate/enolate exists in solution. As such, the difference in reactivity between typical aliphatic amides and oxindole demonstrated by Cu- and Pd-based catalyst systems might not be entirely unexpected.

Since a weak base was employed (K_2CO_3), the large pK_a difference (~5) between oxindole and base indicates that an appreciable quantity of an anionic amidate species does not exist in solution; thus, an intermolecular ligand exchange between an oxindolate anion and XPhos·Pd(Ar)(Cl) **17** is unlikely. As such, it is likely that the oxindole is further acidified by reversible coordination of the Pd(II) intermediate **17** to the oxindole carbonyl to form **18** (Scheme 3). Deprotonation of the acidified oxindole should occur at *N* as opposed to *C3* since deprotonation is kinetically faster from *N*–*H* than from *C*–*H* bonds, in which rehybridization must occur at the carbon atom.²¹ Thus, deprotonation of **18** would initially lead to **6**, followed by an intramolecular migration of Pd from *O* to either *N* or *C*. If intramolecular isomerization is the preferred pathway, then a plausible reaction sequence to form a *C*-bound Pd enolate that does not involve formation a Pd–*N* bond may be **17** → **18** → **6** → **7** → **8** → **2**. If a Pd–*N* bond does transiently form, then the reaction pathway might proceed as such, **17** → **18** → **6** → **5** → **1** → **5** → **6** → **7** → **8** → **2**.

For the Pd-catalyzed *C*-arylation reaction of oxindole with aryl halides, transmetalation of a molecule of oxindole to the $L_1Pd(Ar)(X)$ complex can provide multiple isomeric species. Two of these isomers, namely, **1** and **2**, would reductively eliminate to provide the *N*-aryl and *C3*-aryl oxindole products, respectively. The energy profile illustrating the reaction course with the relative energies of the key intermediates and transition states is shown in Figure 7. The *C3*-aryl product, which is exclusively observed in the Pd-catalyzed reaction, must result from a rapid reductive-elimination from the higher-energy Pd–*C*-bound enolate, **2**, as opposed to the more stable Pd–*N*-bound amidate, **1**. Therefore, the selectivity demonstrated by the Pd-catalyzed reaction is kinetically governed according to the Curtin–Hammett principle.²² The 2.4 kcal/mol difference in energy between **1-TS** and **2-TS** is consistent with the

(16) Paine, A. J. *J. Am. Chem. Soc.* **1987**, *109*, 1496.

(17) Strieter, E. R. Mechanistic Studies on Metal-Catalyzed Carbon–Nitrogen Bond Forming Reactions. Ph.D. Thesis, Massachusetts Institute of Technology, Cambridge, MA, June 2005.

(18) Zhang, S. L.; Liu, L.; Fu, Y.; Guo, Q. X. *Organometallics* **2007**, *26*, 4546.

(19) Arai, S.; Hida, M.; Yamagishi, T. *Bull. Chem. Soc. Jpn.* **1978**, *51*, 277.

(20) (a) Jazdzewski, B. A.; Young, V. G., Jr.; Tolman, W. B. *Chem. Commun. (Cambridge, U.K.)* **1998**, 2521. (b) Näther, C.; Beck, A. *Acta Crystallogr., Sect. E: Struct. Rep. Online* **2004**, *60*, 1008. (c) Blue, E. D.; Davis, A.; Conner, D.; Gunnoe, T. B.; Boyle, P. D.; White, P. S. *J. Am. Chem. Soc.* **2003**, *125*, 9435.

(21) (a) Eigen, M. *Angew. Chem., Int. Ed.* **1964**, *3*, 1. (b) Borwell, F. G.; Boyle, W. J.; Hautala, J. A.; Yee, K. C. *J. Am. Chem. Soc.* **1969**, *91*, 4002. (c) Kresge, A. J. *Acc. Chem. Res.* **1975**, *8*, 354.

(22) Anslyn, E. V.; Dougherty, D. A. *Modern Physical Organic Chemistry*, 3rd ed.; University Science Books: Sausalito, CA, 2006; pp 378–379.

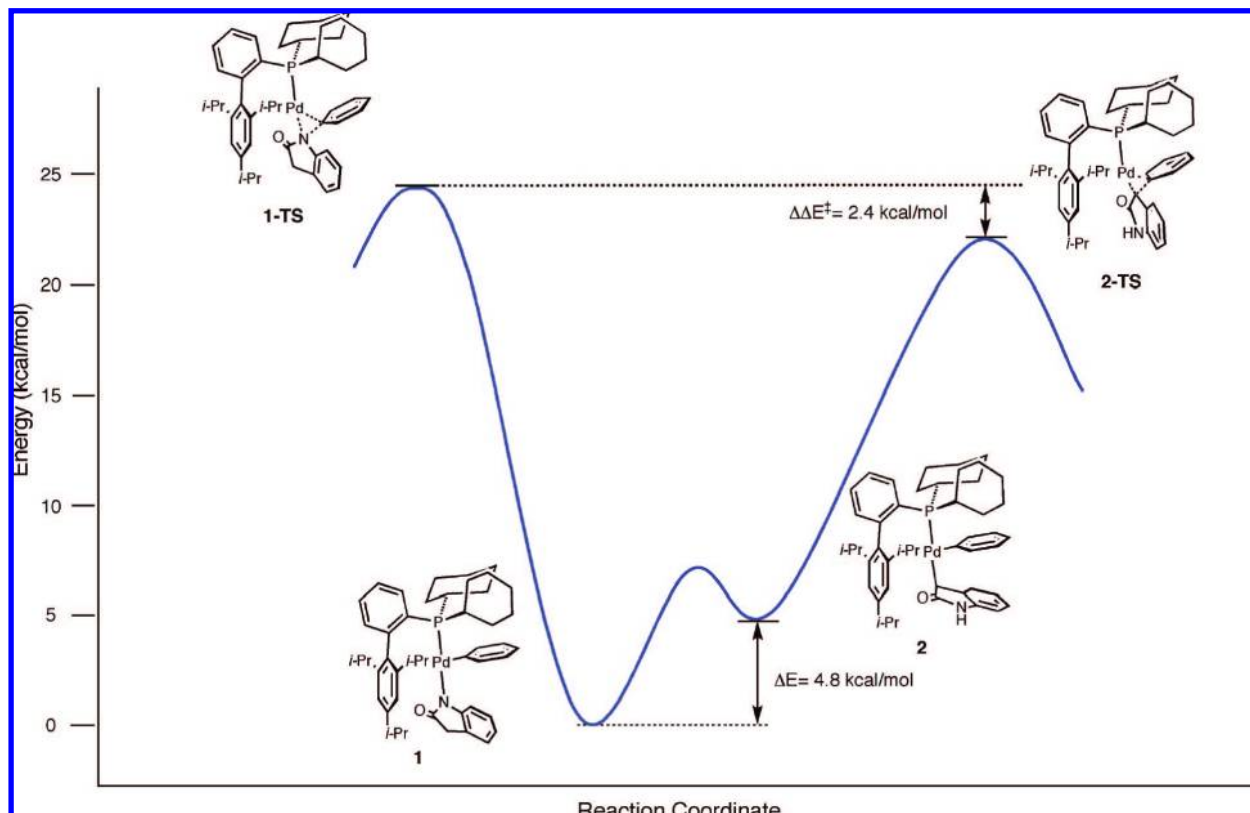
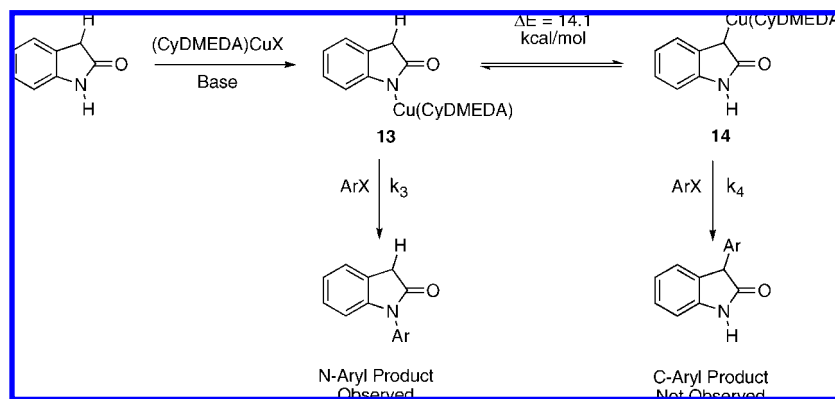


Figure 7. Energy diagram for XPhos•Pd(Ph)(oxindolate) reductive-elimination.

Scheme 4. Mechanistic Considerations for Cu-Catalyzed N-Arylation of Oxindole



observed selectivity of the catalytic reaction. This difference in energy is likely a reflection of the relative electronegativities of nitrogen and carbon and the overlap of the relevant molecular orbitals with those of Pd.²³ Since the halide anion is not present during the proposed selectivity-determining event of the cycle, the change in identity of the electrophile from an aryl chloride to a bromide or sulfonate ester does not have an effect on the chemoselectivity observed in the catalytic reaction (e.g., Table 1, entries 11 and 12). However, the change in the nature of the electrophile should have an effect on the relative rate of reaction.

For the Cu-catalyzed N-arylation reaction, the computational studies of the relevant CyDMEDA-Cu(oxindolate) species suggest that N-bound species **13** is favored by 14.1 kcal/mol over the C-bound isomer **14** (Scheme 4). Therefore, the

selectivity observed for the Cu-catalyzed N-arylation of oxindole might be governed by two different factors: (1) aryl halide activation from **13** proceeds faster than from **14** and/or (2) aryl halide activation proceeds faster than the isomerization process. If the first factor is selectivity-determining, there could be a dynamic equilibrium in solution between **13** and **14**. The nature of the aryl halide activation step in Cu-catalyzed C-heteroatom bond-forming substitution reactions of aryl halides is not well-understood.^{17–19} Kinetic studies for the reaction of 2-pyrrolidinone with 5-iodo-*m*-xylene estimate ΔG^\ddagger to be 19.4 kcal/mol.¹⁷ Therefore, it is plausible that the C-bound enolate does exist in small portions in solution and that the selectivity is governed by the aryl halide activation process ($k_3 > k_4$). If the second factor is selectivity-determining, then the absence of a low energy pathway for the interconversion of **13** and **14** controls the reaction's outcome. A better understanding of the mechanism of aryl halide activation is required to properly

(23) Hartwig, J. F. *Inorg. Chem.* **2007**, *46*, 1936.

estimate the transition state energies for this step and to gain a full understanding for the observed chemoselectivity of the Cu-catalyzed reaction.

Conclusion

In summary, we reported efficient and complementary Pd- and Cu-based catalyst systems for the C3- and N-arylation reactions of unprotected oxindoles using aryl halides. The use of a weak base allows for the presence of a wide variety of functional groups and substitution patterns that are not tolerated with stronger bases.^{7b,c} Theoretical calculations suggest that for both Pd- and Cu-based catalyst systems, the respective metalated oxindoles have a strong preference for the oxindole moiety to coordinate as an N-bound amidate as opposed to a C3-bound enolate. For the Pd-based catalyst system, the energy difference between the Pd-amide and Pd-enolate is ~ 5 kcal/mol; however, the selectivity is governed by rapid C–C reductive-elimination as compared to C–N reductive-elimination based on calculated transition state energies. For the Cu-based catalyst system, the preference for the metal to bind at N1 is stronger (~ 14 kcal/mol). In this case, the selectivity might be governed by rapid aryl halide activation from the diamine-Cu(I)-amidate complex as compared to the diamine-Cu(I)-enolate. Alternatively, a low energy pathway for Cu to isomerize from N to C may not exist, and the C-bound enolate might never form. The implications of this study should be useful for those chemists interested in understanding the inherent differences between Pd- and Cu-based catalyst systems for nucleophilic substitution reactions of aryl halides.

Computational Methods

All calculations were performed with the Gaussian '03²⁴ suite of programs. DFT calculations employed the B3LYP functional²⁵ using the 6-31G(d) basis set for all atoms in the Cu complexes.

(24) Frisch, M. J.; *Gaussian 03*, revision D.01; Gaussian Inc.: Wallingford, CT, 2004.

Because of the size of the XPhos•Pd complexes, geometry optimization was first performed using a two-layered ONIOM²⁶ calculation (B3LYP/6-31g(d):UFF) with oxindole, phenyl, Pd, and P at a high level and the rest of the ligand at a low level. The resulting structures were then reoptimized using all-atom DFT B3LYP/6-31g(d) with the LANL2DZ basis set and the Hay–Wadt effective core potential²⁷ for Pd. To obtain the final ΔE values, single-point energy calculations were performed with the 6-311g(d,p) basis set with implicit solvation included. Frequency calculations were performed on all optimized structures to confirm that the minima had no negative frequencies and that transition states had a single imaginary frequency. The Gibbs free energies were calculated at 298.15 K and 1 atm.

Acknowledgment. We thank the National Institutes of Health (NIH) (GM58160 and GM46059) for financial support of this project. R.A.A. is grateful to Pfizer and the NIH (F31GM081905) for predoctoral fellowships. A.M.H. thanks Aldrich for a Graduate Student Innovation in Organic Chemistry Award. We thank Amgen, Boehringer-Ingelheim, and Merck for additional unrestricted financial contributions. XPhos used for this study was generously provided by Saltigo. The NMR instruments used for this study were furnished by funds from the National Science Foundation (CHE 9808061 and DBI 9729592).

Supporting Information Available: Experimental procedures and characterization data for all new and known compounds, computational data for complexes, and complete ref 24. This material is available free of charge via the Internet at <http://pubs.acs.org>.

JA803179S

- (25) (a) Becke, A. D. *J. Chem. Phys.* **1993**, *98*, 5648. (b) Lee, C.; Yang, W.; Parr, R. G. *Phys. Rev. B: Condens. Matter Mater. Phys.* **1988**, *37*, 785.
- (26) (a) Svensson, M.; Humbel, S.; Froese, R. D. J.; Matsubara, T.; Sieber, S.; Morokuma, K. *J. Phys. Chem.* **1996**, *100*, 19357. (b) Vreven, T.; Morokuma, K.; Farkas, O.; Schlegel, H. B.; Frisch, M. J. *J. Comput. Chem.* **2003**, *24*, 760.
- (27) Hay, P. J.; Wadt, W. R. *J. Chem. Phys.* **1985**, *82*, 299.